

---

# Chapter 3

---

*Magnetic and Dielectric Studies of Barium  
hexaferrite ( $BaFe_{12}O_{19}$ ) Ceramic synthesized by  
chemical route*

---

# ***Magnetic and Dielectric Studies of Barium hexaferrite (BaFe<sub>12</sub>O<sub>19</sub>) Ceramic synthesized by chemical route***

---

## **3.1. Introduction**

Ferromagnetic Oxides (ferrites) were firstly introduced in 1952 and dominated gradually in the field of the permanent magnet. Depending on the crystal structure and chemical formula, hexaferrites are divided into five categories such as W-type (BaMe<sub>2</sub>Fe<sub>16</sub>O<sub>27</sub>), X-type (Ba<sub>2</sub>Me<sub>2</sub>Fe<sub>28</sub>O<sub>46</sub>), Y-type (Ba<sub>2</sub>Me<sub>2</sub>Fe<sub>12</sub>O<sub>22</sub>), Z-type (Ba<sub>3</sub>Me<sub>2</sub>Fe<sub>24</sub>O<sub>41</sub>) and M-type barium hexaferrite, BaFe<sub>12</sub>O<sub>19</sub> (BHF). It exists in different form such as garnets, cubic, hexagonal, orthoferrites. M-type barium hexaferrite acquires an important class of magnetic material due to their electrical and magnetic properties with excellent chemical stability and low-cost production [Özgür *et al.* (2009) (a), Pullar (2012), Özgür and Alivov (2009) (b)]. Ceramic industry requires the materials having high magneto-crystalline anisotropy, high saturation magnetization, high Curie temperature, high coercivity, the high natural resonant frequency with an excellent capability and corrosion resistance [Singhal *et al.* (2011), Onreabroy *et al.* (2012), Zhang *et al.* (2007)]. In addition to this, because of intrinsic magneto- crystalline anisotropy field in BHF ceramic, it can be used at much higher frequency than the ferrites with spinal and garnet structure [Cho and Kim (1999)]. Barium hexaferrite (BaFe<sub>12</sub>O<sub>19</sub>) meets these properties very well, and it becomes one of the most high-tech materials in recent years [Li *et al.* (2012)]. The hexagonal structure of BHF ceramic is an M-type hexaferrite. The synthesis of M-type hexaferrites by several methods such as citrate precursor, hydrothermal, micro- emulsion, glass crystallization, sol–gel, sonochemical, co-precipitation, Nonconventional methods and mechanochemical activation were reported earlier [Sankaranarayanan *et al.* (1993), Wang *et al.* (1993), Xu *et al.* (2008), El-Hilo *et al.* (1994), Sudakar *et al.* (2003), Shafi and Gedanken (1999), Pankov *et al.* (2008), Carp *et al.* (1998), Sharma *et al.* (2007)]. Although ferroelectricity and

# ***Magnetic and Dielectric Studies of Barium hexaferrite (BaFe<sub>12</sub>O<sub>19</sub>) Ceramic synthesized by chemical route***

---

ferromagnetism rarely coexist in these materials [Wang *et al.* (2009)], mostly afford weak ferromagnetism because at room temperature, multiferrorism is essential to understanding for multiferroic devices that exhibits coupling between ferroelectric and ferromagnetic order at ambient condition. M-type hexaferrite has great attentions due to its simplest crystalline structure among hexagonal ferrite and ferromagnetism at room temperature due to the presence of an unpaired electron in d-orbital of iron. It was widely used in various applications like computer data storage, video recorder and disk driver, high-density perpendicular magnetic and magneto-optic recording media [Pfeiffer *et al.* (1993), Rashad *et al.* (2008)]. The electrical properties of the materials as a function of temperature (isothermal), time (isochronal) and frequency are usually referred as regarding dielectric constant, which are important properties of ferrite. The electrical property measurements related to the dielectric loss over a frequency range of 1 MHz–1 GHz. The dielectric constant and loss characteristics of the material are necessary for fabricating electrical and electronic devices [Mallick *et al.* (2007)]. In the present Work, BHF ceramic was synthesized by the chemical method for the improvement of dielectric constant and dielectric loss, microstructural and magnetic properties of the materials.

## **3.2. Experimental**

### **3.2.1. Material synthesis**

Barium hexaferrite was synthesized by chemical route. The starting materials were taken as barium nitrate Ba (NO<sub>3</sub>)<sub>2</sub> (99% Merck, India), iron nitrate Fe (NO<sub>3</sub>)<sub>3</sub> .9H<sub>2</sub>O (98% Merck, India), and citric acid C<sub>6</sub>H<sub>8</sub>O<sub>7</sub> . H<sub>2</sub>O (99% Merck, India). The stoichiometric amount of Ba<sup>+2</sup> and Fe<sup>+3</sup> ions were dissolved in distilled water and per equivalent to metal ions of citric acid was added to this reaction mixture. The obtained reaction mixture was heated on hot plate with continuous stirring at 70–80 °C to evaporate water. After removal of water, a fluffy mass obtained which

## ***Magnetic and Dielectric Studies of Barium hexaferrite (BaFe12O19) Ceramic synthesized by chemical route***

---

was burn with sooty flame at higher temperature. The resulting ash was ground with the help of agate and mortar to make fine powder. The powder was calcined at 850 °C for 8 h. Calcined powder was used to make cylindrical pellets (13 mm × 1.6 mm) with the help of PVA binder on applying 4 tons of pressure for 60 Second. These pellets were sintered at 1050 °C for 12 h and further used for characterization, dielectric and magnetic measurements.

### **3.2.2. Characterization**

The diffraction pattern of sintered BHF ceramic was recorded by X-ray diffractometer (Rigaku miniflex 600, Japan) using Cu-K $\alpha$  radiation ( $\lambda = 1.54 \text{ \AA}$ ) with scan rate of 2°/min. The FTIR spectra of sintered powder was characterized by ATRFTIR (Bruker, ALPHA model) Spectrophotometer using KBr pellets in the frequency range 500–1500 cm<sup>-1</sup>. The surface morphology was observed by scanning electron microscope (ZEISS model, EVO18 Germany) whereas elemental composition was analyzed by EDX (Oxford instrument; USA). The particle size was examined by transmission electron microscope (TEM TECHNAI G2 20 TWIN). For TEM measurement the small amount of sample was dispersed in acetone and sonicated for 30 min. A drop of this solution was put on a carbon-coated copper grid and dried in hot air oven for 1 h. Magnetic measurements were carried out with a Quantum Design MPMS-3, over a temperature range 5–300 K and applied a magnetic field of  $\pm 2$  T. In addition to this, temperature dependent Zero field cooling (ZFC) and field cooling (FC) magnetization were also recorded at 100 Oe applied field using SQUID VSM dc magnetometer in the same temperature range. Silver-coated cylindrical pellets were used for dielectric measurement by LCR meter (PSM 1735, NumetriQN4L U.K.).

# *Magnetic and Dielectric Studies of Barium hexaferrite (BaFe<sub>12</sub>O<sub>19</sub>) Ceramic synthesized by chemical route*

## 3.3. Results and discussion

### 3.3.1. Micro-structural studies

Single-phase formation of BaFe<sub>12</sub>O<sub>19</sub> ceramic sintered at 1050 °C for 12 h is confirmed from XRD pattern shown in Figure 3. 1(a), all diffraction peaks are index with JCPDS file (27– 1029). The diffraction pattern of BHF ceramic sintered at 900 °C for 12 h shown in Figure 3. 1 (b), indicates minor impurity of  $\alpha$ - Fe<sub>2</sub>O<sub>3</sub>with JCPDS file (89–7074) which vanished at 1050 °C for 12 h support single-phase formation.

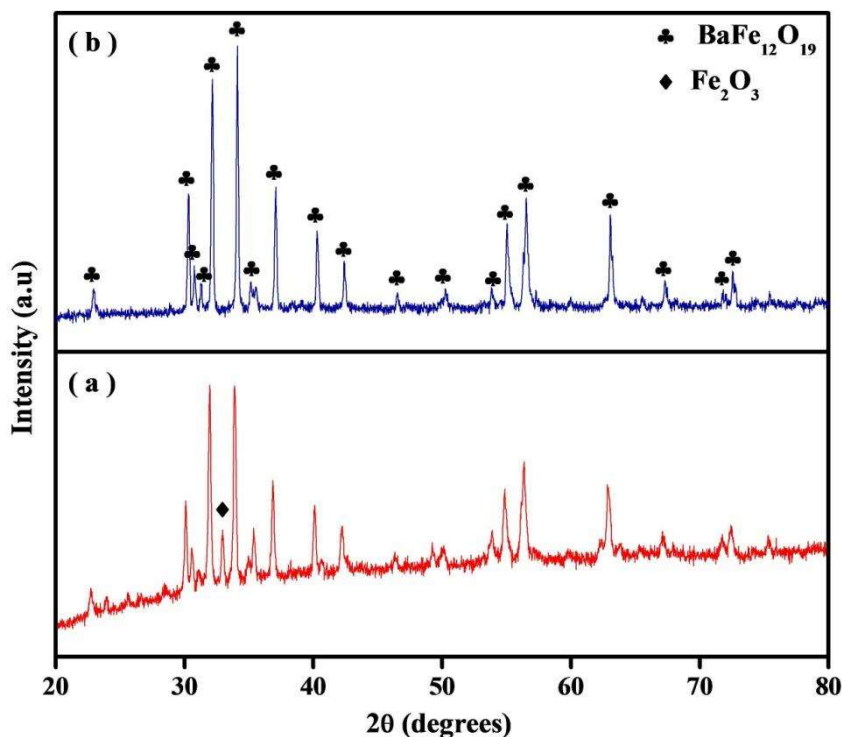


Figure 3.1 (a) and (b) shows XRD diffraction patterns of BHF ceramic sintered at 900 °C and 1050 °C respectively for 12h.

Rietveld refinement data of BHF ceramic showing hexagonal cell with space group P6<sub>3</sub>/mmc shown in Figure 3.2. The lattice parameters are given in table 3.1 and observed cell

## ***Magnetic and Dielectric Studies of Barium hexaferrite (BaFe<sub>12</sub>O<sub>19</sub>) Ceramic synthesized by chemical route***

ratio  $c/a$  is found to be 3.9399 that has been reported earlier [Maswadeh *et al.* (2015)]. Rietveld refinement parameters and atomic positions are shown in Table 3.2.

**Table 3.1** Cell parameters for barium hexaferrite (BaFe<sub>12</sub>O<sub>19</sub>) ceramic.

Cell parameters	$a = b = 5.8860 \text{ \AA}$	$c = 23.1829$
Cell ratio	$c/a = 3.9399$	-
Angle	$\alpha = \beta = 90.0000^\circ$	$\gamma = 120.0000^\circ$
Cell Volume	$695.5767 \text{ \AA}^3$	-

**Table 3.2** Refined structural parameters of BaFe<sub>12</sub>O<sub>19</sub> with Space Group P6<sub>3</sub>/mmc (194), Bragg R-factor: 2.19, RF factor: 2.54,  $\chi^2$ : 1.16.

Atom	Ox	X	Y	Z
Ba	+2	0.66667	0.33333	0.25000
Fe 1	+3	0.00000	0.00000	0.00000
Fe 2	+3	0.00000	0.00000	0.26100
Fe 3	+3	0.33333	0.66667	0.02700
Fe 4	+3	0.33333	0.66667	0.19010
Fe 5	+3	0.17000	0.34000	0.10850
O 1	-2	0.00000	0.00000	0.14400
O 2	-2	0.33333	0.66667	0.05500
O 3	-2	0.18600	0.37300	0.25000
O 4	-2	0.16800	0.33700	0.05210
O 5	-2	0.51400	0.02800	0.15190

## *Magnetic and Dielectric Studies of Barium hexaferrite (BaFe12O19) Ceramic synthesized by chemical route*

---

It is observed from the Table that the oxidation state of Fe is +3 only, which is occupied five different planes of the hexagonal unit cell.

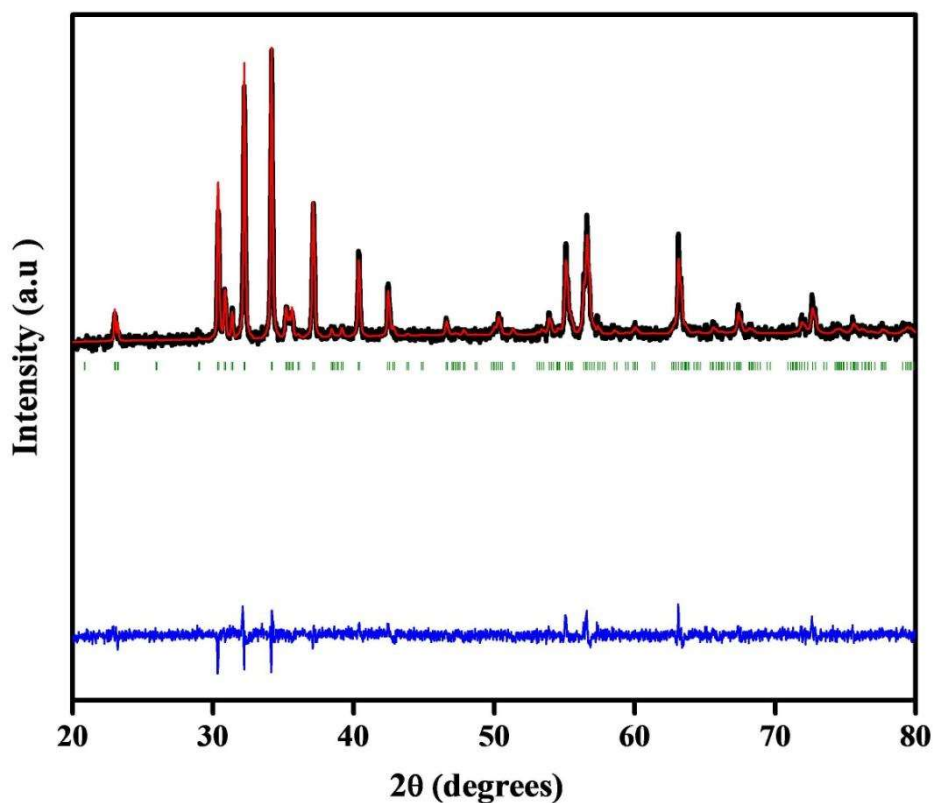


**Figure 3.2** Experimentally observed (black line), Rietveld calculated (red line) and their difference (blue bottom line) profile obtained after Rietveld analysis of XRD data for BHF ceramic using hexagonal structure in the space group  $P6_3/mmc$ . The vertical tick marks above the bottom line show peak position.

The average crystallite size was calculated by taking the most intense peaks of BHF ceramic using the Debye Scherrer formula.

$$D = k\lambda/\beta \cos\theta \quad (3.2)$$

## ***Magnetic and Dielectric Studies of Barium hexaferrite (BaFe<sub>12</sub>O<sub>19</sub>) Ceramic synthesized by chemical route***

---

where,  $k$  is the shape coefficient value taken as 0.90,  $\lambda$  is the wavelength of X-ray,  $\theta$  is the diffraction angle, and  $\beta$  is the peak width of the diffraction peak at half-maxima (FWHM) in radians. The  $\beta$  is corrected value of diffraction peak due to instrumental broadening for crystallite size with reference to standard silicon wafer sample. The average crystallite size of BHF ceramic is found to be 59.83 nm.

Figure 3.3 shows the FTIR spectra of the BHF ceramic sintered at 1050 °C for 12 h, recorded in the frequency range 500–1500  $\text{cm}^{-1}$ . Two absorption peaks at 540 and 575  $\text{cm}^{-1}$  represents Fe-O stretching vibration bands corresponding to octahedral and tetrahedral sites in the BHF ceramic.

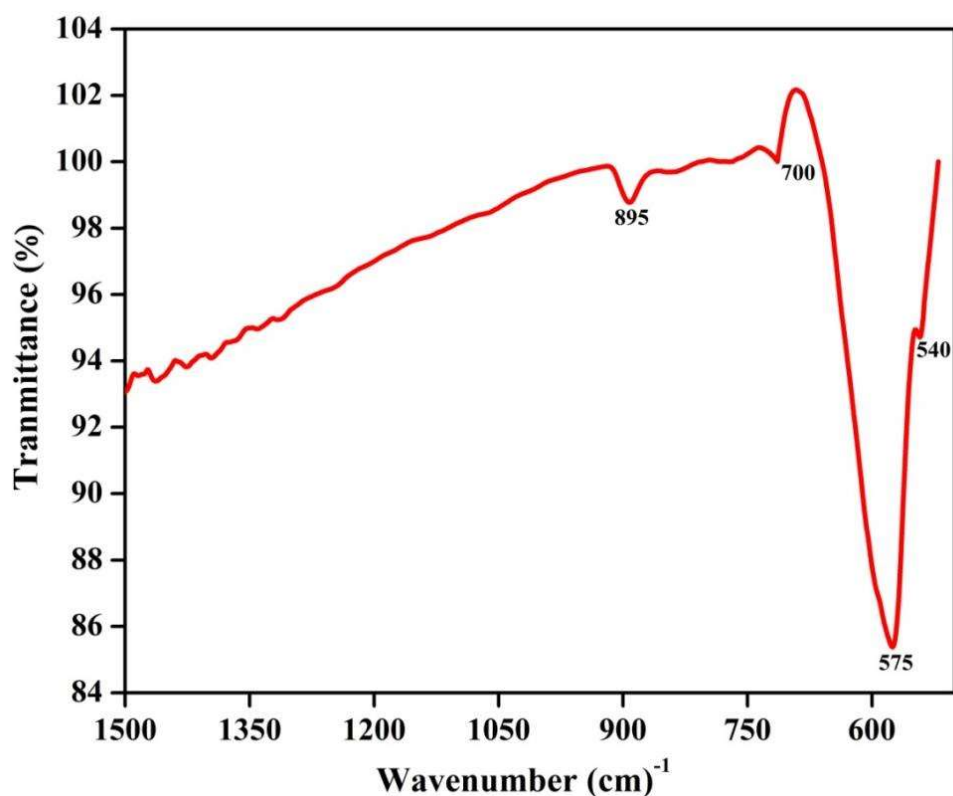


**Figure 3.3** FTIR spectra of BHF ceramic sintered at 1050 °C for 12 h.

## ***Magnetic and Dielectric Studies of Barium hexaferrite (BaFe<sub>12</sub>O<sub>19</sub>) Ceramic synthesized by chemical route***

---

The Ba-O bands also present at  $895\text{ cm}^{-1}$  and Fe-O-Fe bands observed in between  $1100$  and  $1500\text{ cm}^{-1}$  which gives the qualitative information about metal oxide bonds of the BHF ceramic [Gordani *et al.* (2014)].

The bright field TEM image of the BaFe<sub>12</sub>O<sub>19</sub> ceramic sintered at  $1050\text{ }^{\circ}\text{C}$  for 12 h is shown in Figure 3.4(a, b).

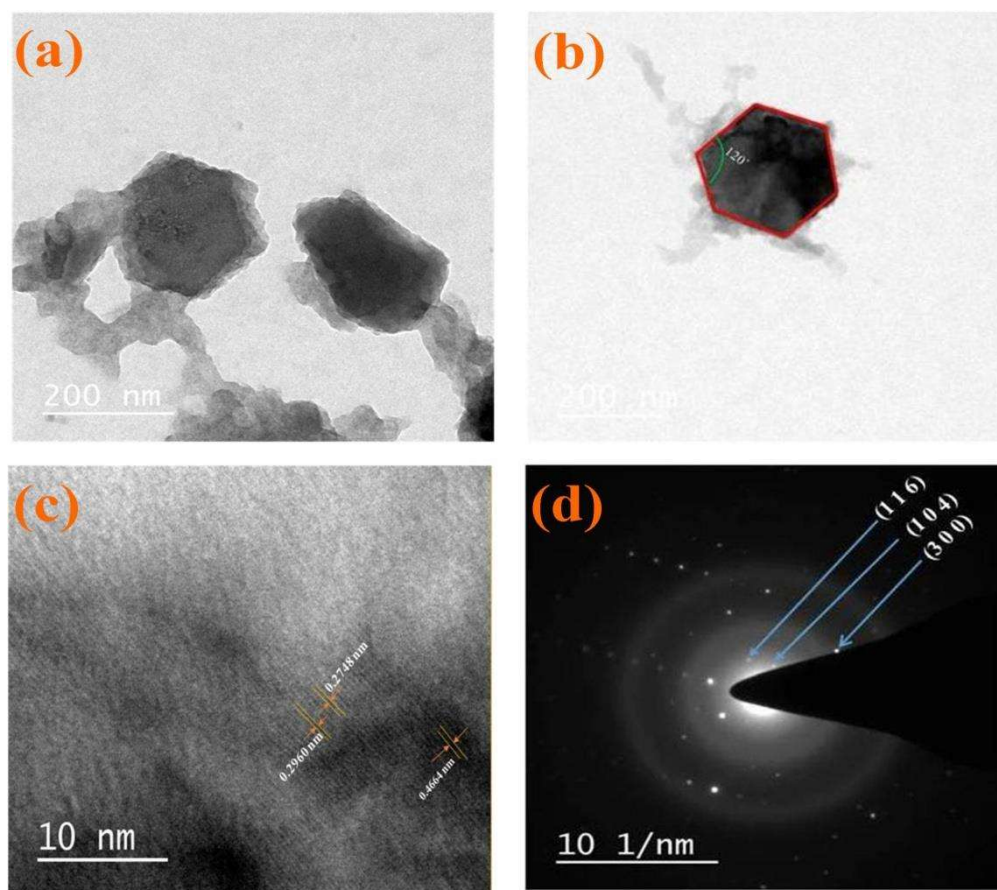


**Figure 3.4**(a) Bright field TEM image (b) Single hexagonal particle having characteristic hexagonal bond angle  $120^{\circ}$  (c) High-resolution TEM image with d spacing (d) Selected area diffraction (SAED) pattern of BHF ceramic.



## ***Magnetic and Dielectric Studies of Barium hexaferrite (BaFe<sub>12</sub>O<sub>19</sub>) Ceramic synthesized by chemical route***

---

The calculated average grain size of the BHF ceramic is in the range 0.3–1.0  $\mu\text{m}$ . Grain size obtained by SEM analysis is larger than that of crystallite size calculated from XRD measurement. The higher grain size is explained due to its formation by combination of few particles. The EDX spectrum of the BHF ceramic corresponding to the SEM images shown in Figure 3.5(b), confirms the presence of Ba, Fe, and O elements. The quantitative atomic percentage data of Ba, Fe, and O in BHF ceramic obtained from EDX data, are 2.94, 32.13, and 64.93 respectively. The observed atomic percentage data confirms the molecular formula as per their stoichiometric ratio.

Figure 3.6 (a) shows the clear grain boundaries with a comparable grain size of the BHF ceramic.

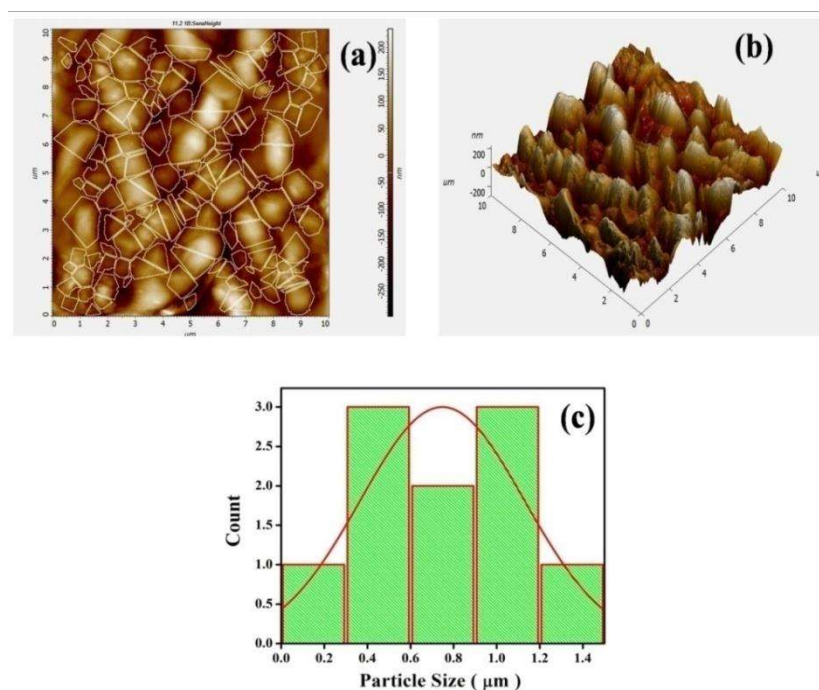


**Figure 3.6** AFM images (a) 2D for grain boundaries (b) 3D for surface roughness and (c) Histogram graph for particle size distribution of BHF ceramic sintered at 1050  $^{\circ}\text{C}$  for 12 h.

## *Magnetic and Dielectric Studies of Barium hexaferrite (BaFe<sub>12</sub>O<sub>19</sub>) Ceramic synthesized by chemical route*

---

The average roughness (Ra) and root mean square (Rq) data are obtained as 44.025 nm and 61.048 nm, respectively on scanned area 11 mm × 11 mm. The distribution of particles on the surface is also recorded by the three dimensional image shown in Figure 3.6 (b). The maximum peak-valley depth of two-dimensional structures is found to be 164.743 nm. Figure 3.6(c) reveals the histogram of grain size indicates the most of the grain are in size range of 300–600 nm, which substantiate with SEM results as mentioned earlier.

### 3.4. Ferroelectric Properties

Figure 3.7 shows polarization verses electric field (P-E) hysteresis loop for BHF ceramic were measured at few selected temperatures.

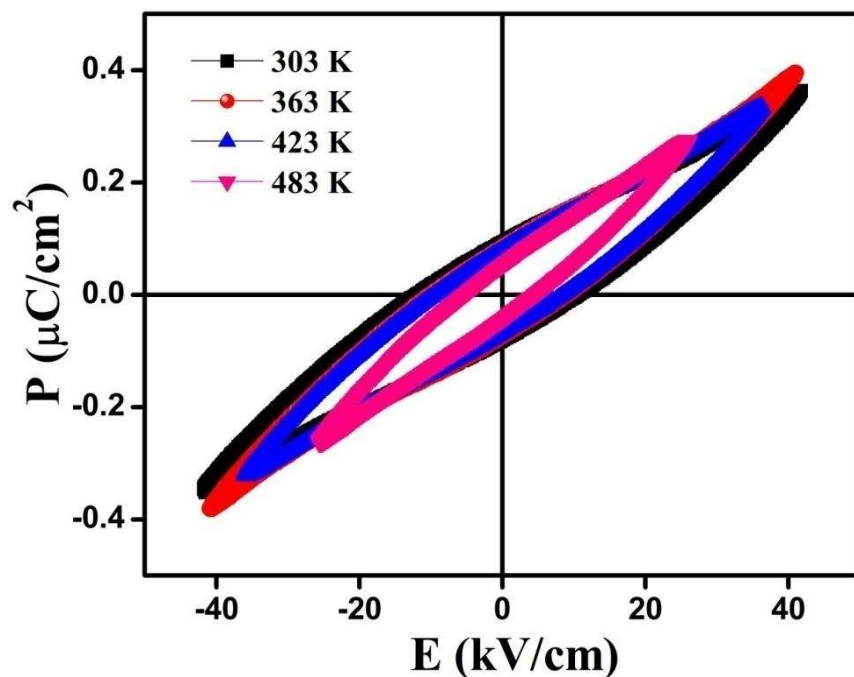


**Figure 3.7** P–E hysteresis loops for barium hexaferrite (BHF) ceramic at few selected temperatures.

## ***Magnetic and Dielectric Studies of Barium hexaferrite (BaFe12O19) Ceramic synthesized by chemical route***

---

These measurements were performed at 100 Hz frequency and on applying electric field 9 kV/cm. It is observed from the figure that both the value of remnant polarization ( $P_r$ ) and coercivity ( $E_c$ ) decreases with increasing temperature corresponding to given electric fields which were summarized in the table 3.3. The decrease in polarization with increasing of temperature was occurred because of switching of dipoles with increase of temperature due to oppose of electric field. The absence of saturation polarization were observed in the P-E hysteresis even applying high electric field that may be due to combined effect parallel joint resistor and capacitor that implies lossy capacitor nature of the materials.

**Table 3.3** Remnant polarization ( $P_r$ ) and Coercivity ( $E_c$ ) of BHFC ceramic at few selected temperatures.

Temperature (K)	Remnant polarization ( $\mu\text{C}/\text{cm}^2$ )	Coercivity (kV/cm)
303	0.093	11.291
363	0.085	9.628
423	0.077	8.426
483	0.054	4.756

### **3.5. Magnetic Properties**

Figure 3.8(a) shows the magnetization curve of zero fields cooled (ZFC) and field cooled (FC) at the temperature of 5– 300 K with the applied magnetic field 100 Oe. The magnetization on both ZFC and FC curves monotonically increases with decreasing temperature, and remains constant from 50 to 5 K. The FC and ZFC curve merged to each other, which clearly revealed that presence of only one magnetic phase and absence of spin-glass transition [Martinez *et al.*

## *Magnetic and Dielectric Studies of Barium hexaferrite (BaFe<sub>12</sub>O<sub>19</sub>) Ceramic synthesized by chemical route*

(1998)]. The M-H hysteresis loops recorded at  $\pm 2$  T for 5 and 300 K shown in Figure 3.8(b). The remnant and saturation magnetization increases with decrease of temperature. The coercivity of material is relatively lower as reported earlier due to distribution of hexagonal particle is not homogeneous throughout the material [Kubo *et al.* (1985)]. Saturation magnetization are found to be 137.97 and 101.23 emu/g for 5 K and 300 K, respectively and these values are higher than the theoretical value due to high phase purity and well-defined crystallinity of BaFe<sub>12</sub>O<sub>19</sub> phase [Shhirk *et al.* (1969)].

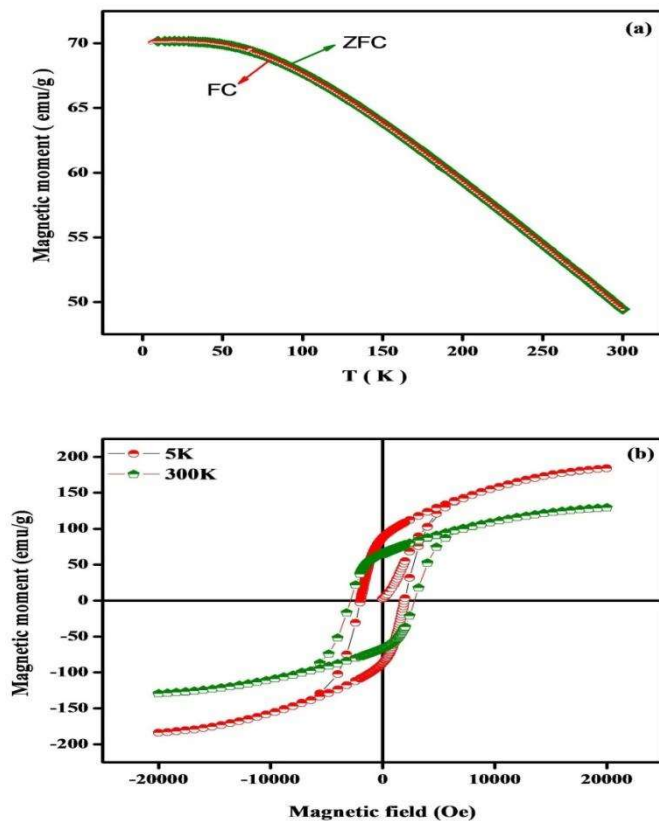


**Figure 3.8** (a) Temperature-dependent ZFC and FC at H=100 Oe (b) M-H hysteresis at 5 and 300 K for the BHF ceramic.

## ***Magnetic and Dielectric Studies of Barium hexaferrite (BaFe<sub>12</sub>O<sub>19</sub>) Ceramic synthesized by chemical route***

---

The squareness ratio ( $M_r/M_s$ ) is close to 0.6 for both temperatures, which indicates single domain crystal structure hard magnetic nature and material is used as permanent magnet as well as magnetic recording devices. The magnetic parameters are mentioned in table 3.4.

**Table 3.4** Magnetic parameters of BaFe<sub>12</sub>O<sub>19</sub> ceramic at different temperature.

T ( K )	M <sub>s</sub> ( emu/g )	M <sub>r</sub> ( emu/g )	M <sub>r</sub> /M <sub>s</sub>	H <sub>c</sub> ( A/m )
5	137.97	86.34	0.625	1.48 × 10 <sup>5</sup>
300	101.23	64.21	0.634	2.24 × 10 <sup>5</sup>

The temperature dependence of inverse magnetic susceptibility for the BHF ceramic depicts in Figure 3.9. The observed fitted plot follows the path of Curie –Weiss law, as represented in Eq. (3.2)

$$\chi = \frac{C}{T-\theta} \quad (3.2)$$

where  $\chi$ , C,  $\theta$  and T represents magnetic susceptibility, Curie constant and Curie-Weiss temperature and temperature, respectively. The experimental values of C and  $\theta$  are calculated and found to be 285.0 emu g<sup>-1</sup> Oe<sup>-1</sup> and 82 K. The positive value of Curie–Weiss temperature ( $\theta$ ) emphasize that the BHF ceramics have ferromagnetic character [Azcondo *et al.* (2015)].

## *Magnetic and Dielectric Studies of Barium hexaferrite (BaFe<sub>12</sub>O<sub>19</sub>) Ceramic synthesized by chemical route*

---

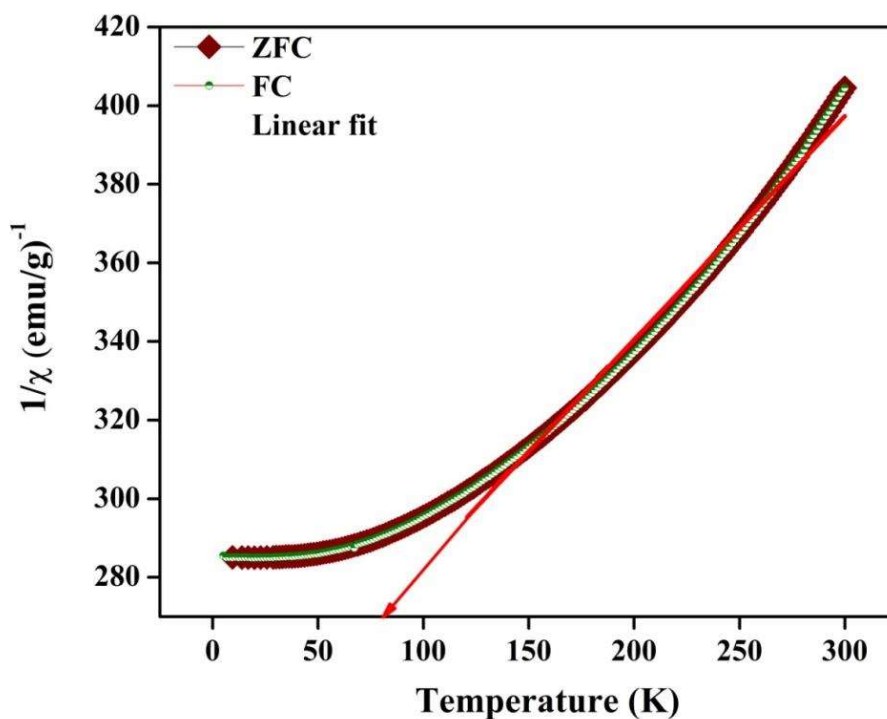


**Figure 3.9** Plots of inverse magnetic susceptibility as a function of temperature recorded at  $\pm 2$  T and applied magnetic field  $H = 100$  Oe

### **3.6. Electrical Properties**

The dielectric dispersion, as well as the formation of inter barrier layer due to grain and grain boundary contribution in the BHF ceramic, can be understood by complex impedance spectroscopy (CIS) which provides the idea about an occurrence of the multi-polarization process and their relaxation conditions. The effective contribution due to grain, grain boundary and electrode interface can be determined by impedance plane plots. It differentiates grains, grain boundaries and electrode contributions by semicircular arcs. Semicircular arcs at low, middle and higher frequency side due to electrode, grain boundary and grain contributions, respectively. The complex impedance plots of the BHF ceramic sintered for 12 h

***Magnetic and Dielectric Studies of Barium hexaferrite (BaFe12O19)  
Ceramic synthesized by chemical route***

---

at few selected temperature (303–483 K) is shown in Figure 3.10 (a) that reveals the presence of two semicircular arcs with different intercepts, which may be due to grain and grain boundary.

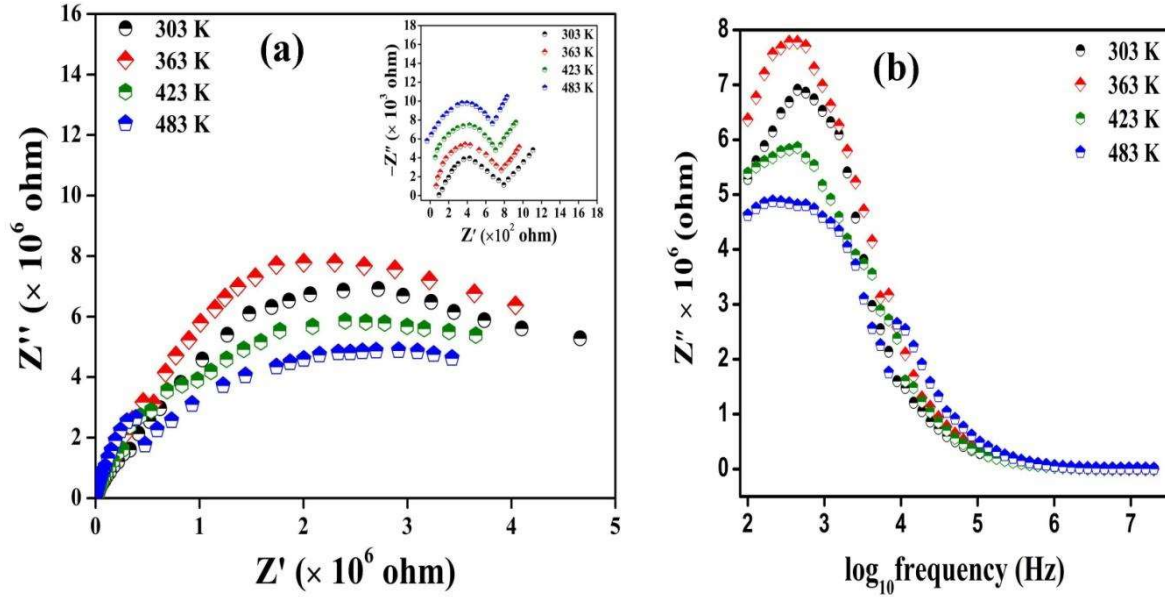


**Figure 3.10** (a) complex Impedance plane plots ( $Z'$  vs  $Z''$ ) at few selected temperature (b) Plots of imaginary impedance ( $Z''$ ) with frequency at few selected temperatures for BHF ceramic sintered at 1050 °C for 12 h.

The expanded view of impedance plots at higher frequency region is shown in the inset of Figure 3.10 (a), which suggests that the intercept on  $Z'$  axis possess through origin explain the existence of grain at the higher frequency region. The first and second semicircle arcs are represent grains resistance ( $R_g$ ) and grain boundary resistance ( $R_{gb}$ ), respectively. The Impedance of grains and grain boundaries is represented by the Eq. (3.3)

$$Z^* = \frac{1}{R_g^{-1} + i\omega C_g} + \frac{1}{R_{gb}^{-1} + i\omega C_{gb}} = Z' - iZ'' \quad (3.3)$$

## ***Magnetic and Dielectric Studies of Barium hexaferrite (BaFe<sub>12</sub>O<sub>19</sub>) Ceramic synthesized by chemical route***

---

Where

$$Z' = \frac{R_g}{1+(\omega R_g C_g)^2} + \frac{R_{gb}}{1+(\omega R_{gb} C_{gb})^2}$$

And

$$Z'' = R_g \left[ \frac{\omega R_g C_g}{1+(\omega R_g C_g)^2} \right] + R_{gb} \left[ \frac{\omega R_{gb} C_{gb}}{1+(\omega R_{gb} C_{gb})^2} \right]$$

The values of grain and grain boundary resistance are calculated and mentioned in table 3.5. It is clear that resistance of grains and grain boundaries decrease with increasing temperature. The suppression of grains occur at higher frequency region due to the higher value of grain boundaries resistance which is usually referred to IBLC mechanism that explains the conducting nature of grains with insulating grain boundaries [Sharma *et al.* (2014)].

**Table 3.5** Calculated values of resistance (R) and capacitance (C) of grain and grain boundary at few selected temperature for barium hexaferrite (BaFe<sub>12</sub>O<sub>19</sub>) ceramic.

Temperature(K)	R <sub>g</sub> (ohm)	R <sub>gb</sub> (ohm)	C <sub>g</sub> (pF)	C <sub>gb</sub> (pF)
303 K	849.25	4796430	0.120	0.581
363 K	790.45	4201259	0.166	0.849
423 K	728.99	3748787	0.230	1.223
483 K	638.69	3467455	0.337	1.695

## *Magnetic and Dielectric Studies of Barium hexaferrite (BaFe12O19) Ceramic synthesized by chemical route*

The variation of imaginary impedance ( $Z''$ ) with frequency at few selected temperatures is shown in Figure 3.10(b). The figure reveals that  $Z''$  decreases with increasing frequency and merge to each other in the higher frequency region. The relaxation peaks observed at lower frequency regions and suppression of peaks at higher frequency explain temperature-dependent thermally assisted ionic phenomenon of the BHF ceramic.

Frequency dependent dielectric constants ( $\epsilon'$ ) at a few selected temperatures are shown in Figure 3.11(a). The dielectric constant below 10 kHz increases with decrease in frequency and remains constant from 10 kHz to 20 MHz. The decreasing behavior of dielectric constant with frequency is explained by Maxwell–Wagner phenomena, which arises due to inhomogeneity in conductivity of grains and grain boundaries at the interface [George *et al.* (2007), Koops (1951)].

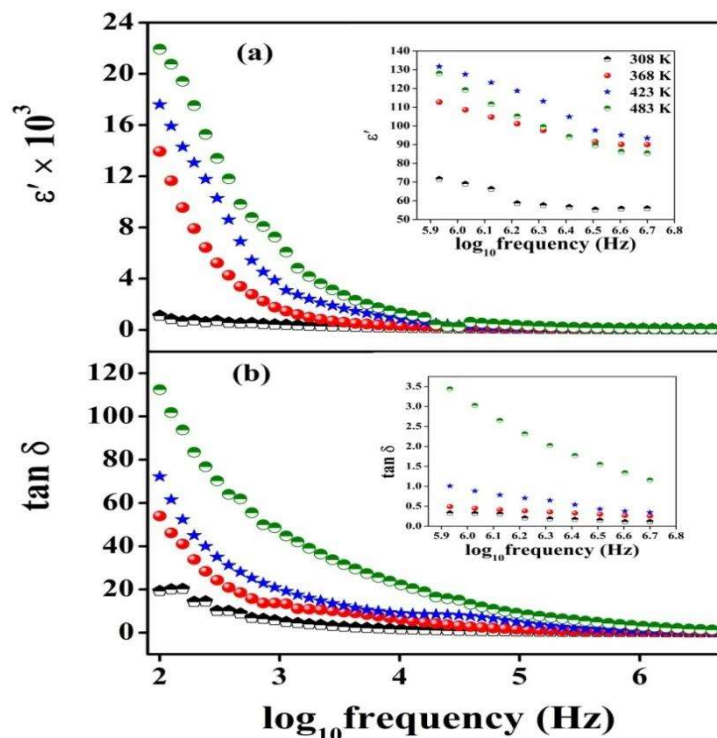


**Figure 3.11** (a) dielectric constant ( $\epsilon'$ ) and (b) dielectric loss ( $\tan \delta$ ) as a function of frequency at few selected temperatures

## *Magnetic and Dielectric Studies of Barium hexaferrite (BaFe12O19) Ceramic synthesized by chemical route*

The value of dielectric constant is found in order of  $\sim 10^3$  at 483 K and 100 Hz. The logarithmic scale of dielectric constant at higher frequency region is shown in the inset of Figure 3.11(a) which shows the clear vision of dielectric constant at higher frequencies. Figure 3.11 (b) shows variation in dielectric loss ( $\tan \delta$ ) as a function of frequency ( $10^2$ - $10^7$  Hz) at few selected temperatures. The values of  $\tan \delta$  are found to be 19, 53, 72, and 111 at temperature 303 K, 383 K, 423 K, 483 K and 100 Hz respectively. The values of  $\tan \delta$  are almost independent in the higher frequency range ( $10^5$ - $10^7$  Hz) and show low value of  $\tan \delta$  (0.9) as indicated in the inset.

Figure 3.12 indicates the variation of dielectric constant ( $\epsilon'$ ) and dielectric loss ( $\tan \delta$ ) with the temperature at few selected frequencies.

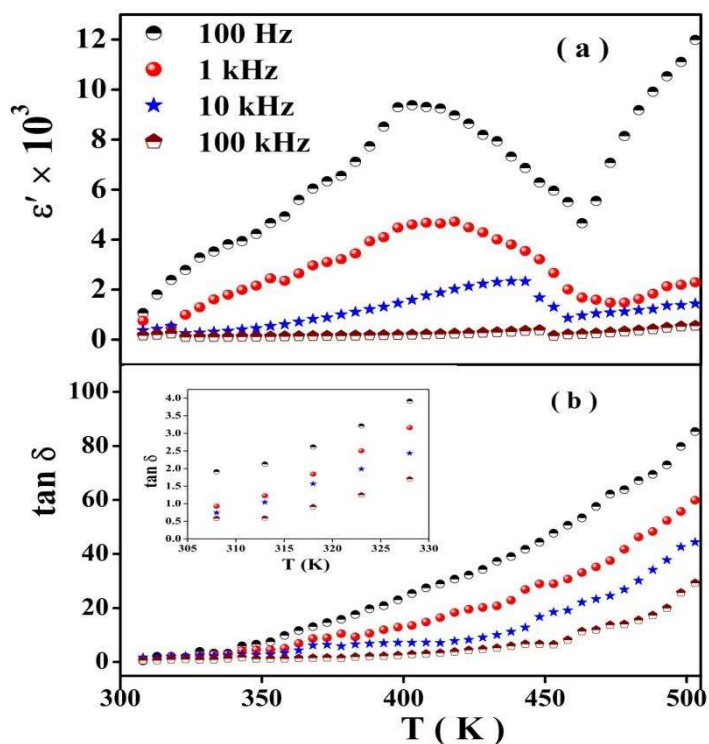


**Figure 3.12** Temperature dependent (a) dielectric constant ( $\epsilon'$ ) and (b) dielectric loss ( $\tan \delta$ ) at few selected frequencies

## ***Magnetic and Dielectric Studies of Barium hexaferrite (BaFe12O19) Ceramic synthesized by chemical route***

Relaxation peaks are observed at 100 Hz, 1 kHz and 10 kHz at 400 K, which shift towards high temperature range so the Curie temperature also increases with frequency [Mu *et al.* (2009)]. Figure 3.12(b) shows that dielectric loss ( $\tan \delta$ ) of the BHF ceramic increases with increase in temperature. A rapid increase in  $\tan \delta$  at higher temperature is due to the exponential enhancement in conductivity with temperature, which arises due to oxygen vacancy present in BHF ceramics during the sintering process [Yadava *et al.* (2016), Khare *et al.* (2016), Singh *et al.* (2016), Gautam *et al.* (2017)].

The dependence of imaginary dielectric constant ( $\epsilon''$ ) on frequency at few selected temperature for the BHF ceramic is shown in Figure 3.13.

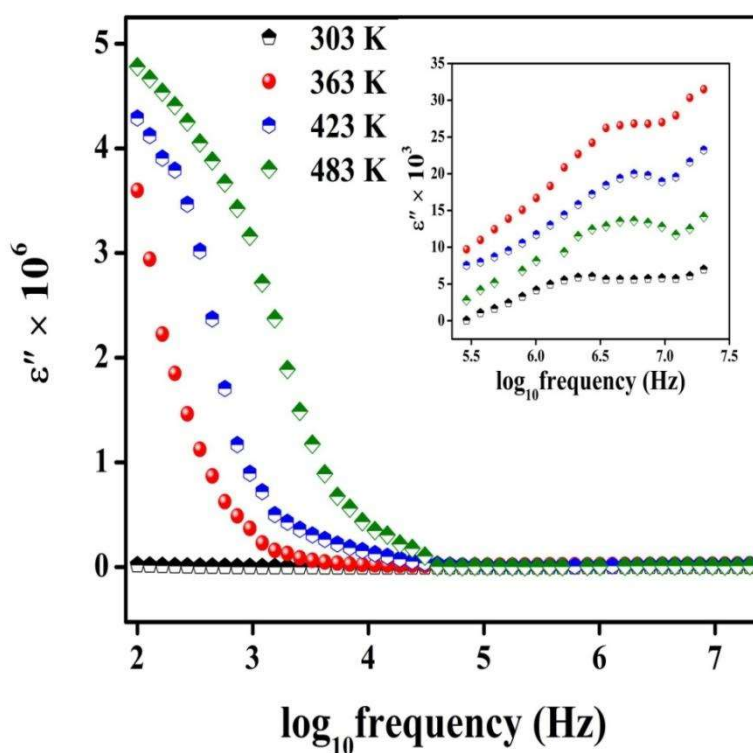


**Figure 3.13** Plots of Imaginary dielectric constant ( $\epsilon''$ ) vs frequency at few selected temperature sintered at 1050 °C for 12 h

## ***Magnetic and Dielectric Studies of Barium hexaferrite (BaFe12O19) Ceramic synthesized by chemical route***

---

It exhibits higher values of ( $\epsilon''$ ) at the lower frequency and higher temperature and rapidly decreases with increasing frequency. The dielectric constant decreases with increasing frequency may be Maxwell interfacial polarization. The constant value of  $\epsilon''$  in the higher frequency region occurs due to periodic reversal of the field so that no charge accumulation at the interface. Impedance studies also clarify lower and the higher resistance value of grain and insulating grain boundary with different conductivity, which causes inhomogeneity in the BHF ceramic.

The imaginary part of dielectric constant ( $\epsilon''$ ) as a function of frequency related with Maxwell–Wagner expressed as the following Eq. (3.4)

$$\epsilon'' = \frac{1}{\omega C_0 (R_{gb} + R_g)} \frac{1 - \omega^2 \tau_{gb} \tau_g + \omega^2 \tau (\tau_{gb} + \tau_g)}{1 + \omega^2 \tau^2} \quad (3.4)$$

Where,

$$\tau_g = C_g R_g \text{ and } \tau_{gb} = C_{gb} R_{gb}$$

$$\tau = \frac{\tau_{gb} R_g + \tau_g R_{gb}}{R_{gb} + R_g}, C_0 = \epsilon_0 \frac{l}{A}$$

where, subscript g and gb represents grains and grain boundaries, respectively,  $\tau$  is the relaxation time,  $\omega$  is the angular frequency,  $l$  and  $A$  are thickness and area of the cylindrical pellets. The Maxwell -Wagner relaxation is clearly shown in inset of the figure at higher frequency region [Wang *et al.* (2017)].

The conductivity ( $\sigma$ ) associated with AC and DC contribution on frequency is expressed by the equation.

$$\sigma = \sigma_{dc} + \sigma_{ac} = \sigma_{dc} + A\omega^s \quad (3.5)$$

## *Magnetic and Dielectric Studies of Barium hexaferrite (BaFe12O19) Ceramic synthesized by chemical route*

At higher frequencies, conductivity obeys Jonscher's law  $\sigma(\omega) \propto \omega^s$  where  $s < 1$  [Dyre and Schroder (2000)]. Where A is the pre-exponential factor,  $\omega$  is angular frequency,  $\sigma_{dc}$  and  $\sigma_{ac}$  are the frequency independent conductivity (DC) and frequency dependent conductivity (AC), and s is the dimensionless frequency exponent parameters. Figure 3.14 shows frequency dependence of AC conductivity at few selected temperatures.

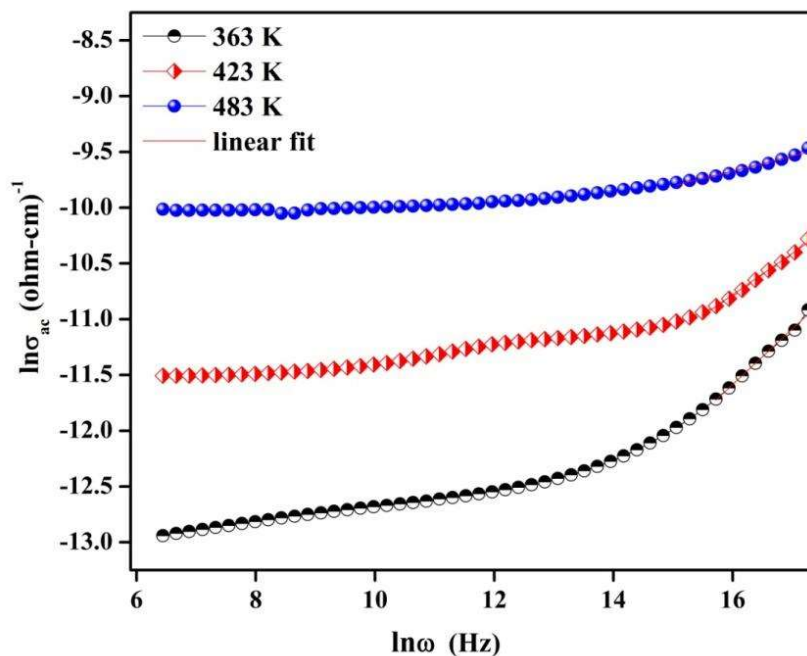


**Figure 3.14** Frequency dependent AC conductivity at few selected temperatures

The critical frequency ( $\omega_c$ ) is found to be 15.06 Hz. The value of frequency exponent parameter (s) obtained from the slope of the plot ( $\ln \sigma$  vs.  $\ln \omega$ ) for BHF ceramic are found to be 0.50, 0.37, and 0.13 at the temperature 363, 423 and 483 K respectively. Such frequency dependent conductivity explained regarding Correlated Barrier Hopping (CBH) model, given by Elliot for crystalline oxide materials [Elliott (1994)].

## ***Magnetic and Dielectric Studies of Barium hexaferrite (BaFe12O19) Ceramic synthesized by chemical route***

---

Figure 3.15 shows the temperature - dependent conductivity at different frequencies. It reveals from figure that conductivity increases with increase in temperature, which suggests that at lower temperature region DC conductivity predominant over AC conductivity because  $\sigma_{ac}$  considerably depends on the frequency. As temperature increases dielectric relaxation takes place, which reduces the frequency dependence of AC conductivity. Therefore, conductivity mainly depends on temperature. According to Arrhenius law, temperature dependent conductivity ( $\sigma$ ) expressed by the following equation

$$\sigma = \sigma_0 e^{-E_a/kT} \quad (3.6)$$

where,  $E_a$  is the activation energy for ionic conduction,  $\sigma_0$  pre-exponential factor  $k$  is the Boltzmann constant, and  $T$  is the absolute temperature. Two different slopes are observed corresponds to lower and higher temperatures. The activation energy in the high-temperature region is found to be 0.46 eV in all measured frequencies. At higher temperature, AC and DC remains same due to curves are merge to each and onset of intrinsic conductivity take place [Prasad *et al.* (2001)]. At lower temperature region the activation energy ( $E_a$ ) of BHF ceramic are found to be 0.50, 0.48, 0.45 and 0.29 eV at 100 Hz, 1 kHz, 10 kHz, and 100 kHz respectively.

## *Magnetic and Dielectric Studies of Barium hexaferrite (BaFe<sub>12</sub>O<sub>19</sub>) Ceramic synthesized by chemical route*

---

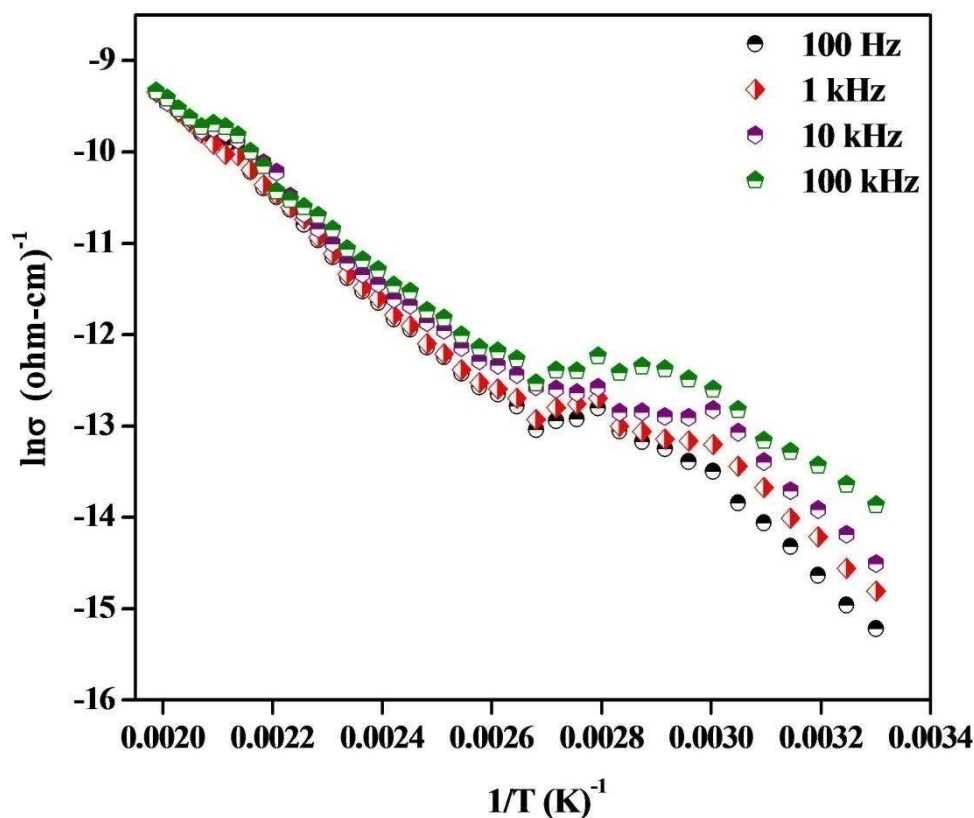


**Figure 3.15** Plots of conductivity with inverse of temperature at few selected frequencies

It is seen that  $E_a$  decrease with increasing frequency, which may be due to enhancement of electronic jumps between two sites on increasing of applied frequency. The lower value of activation energy observed at the higher frequency due to hopping charge mechanism between  $\text{Fe}^{+3}$  and  $\text{Fe}^{+2}$  ions which increase conductivity.

### **3.7. Conclusions**

Hexagonal BHF ceramic was synthesized by the chemical method sintered at 1050 °C for 12 h. XRD confirmed the single phase without any signature of the secondary phase. The structure,

## ***Magnetic and Dielectric Studies of Barium hexaferrite (BaFe<sub>12</sub>O<sub>19</sub>) Ceramic synthesized by chemical route***

---

chemical composition, and microstructure were examined using XRD, EDX and SEM analysis. Rietveld refinement analysis confirms hexagonal structure of BHF ceramic with space group P6<sub>3</sub>/mmc (194) and lattice parameter  $a = b = 5.895 \text{ \AA}$  and  $c = 23.199 \text{ \AA}$ . This material exhibits excellent dielectric and magnetic properties. The value of dielectric constant was found to be very high ( $\epsilon' \sim 22 \times 10^3$ ) at 100 Hz, and 483 K. Magnetic hysteresis loop shows the ferromagnetic to the paramagnetic behavior of material on increasing temperature. Larger the value of squareness ( $M_r/M_s$ ) ratio obtained from hysteresis loop of this ceramic justifies its suitability in various applications such as high magnetic recording media and the permanent magnet. The temperature dependent AC conductivity and frequency exponent parameters ( $s$ ) were interpreted in the terms of Correlated Barrier Hopping (CBH) model.

---

# Chapter 4

---

*Electrical, Magnetic and Dielectric properties of  
cobalt doped barium hexaferrite  $BaFe_{12-x}Co_xO_{19}$   
( $x=0.0,0.05,0.1,$ and $0.2$ ) Ceramic Prepared via  
Chemical route*

---